



OPEN Age-related changes in the cytoplasmic ultrastructure of feline oocytes

Brańiel Natalia¹✉, Perrin John¹, Młodawska Wiesława³, Niżański Wojciech¹, Podhorska-Okołów Marzenna^{2,4}, Haczkiwicz-Leśniak Katarzyna², Kulus Michał²✉ & Ochota Małgorzata¹✉

This study elucidates the impact of aging on the cellular architecture of feline oocytes, with a particular emphasis on organelles essential for fertilization and embryo development. Using transmission electron microscopy (TEM), the research compares oocytes from prepubescent, cycling adult, and aged cats, revealing notable differences in the arrangement of key structures, particularly mitochondria, lipid droplets, and vacuoles. Oocytes from adult donors are at their metabolic peak, demonstrating a higher concentration of mitochondria near lipid droplets, supporting efficient energy metabolism. In contrast, younger and older oocytes exhibit larger lipid droplets and reduced mitochondrial density, indicative of diminished metabolic activity. These findings not only underscore the necessity of selecting an optimal donor age for in vitro fertilization but also suggest potential biomarkers for oocyte quality assessment. This novel insight offers promising strategies to enhance reproductive success, improve assisted reproduction outcomes, and support feline conservation efforts.

Keywords Oocytes, Electron microscopy, Reproductive biology, Fertility, Cats, Aging

The morphology and behavior of oocyte cytoplasmic organelles have been extensively studied in humans, mice, and several other species^{1,2}. However, research on cats remains limited^{3–5}. Moreover, the ultrastructural characteristics of feline oocytes of varying quality are poorly understood and remain largely unexplored. Key organelles, such as mitochondria (Mt), cortical granules (CGs), and lipid droplets (LDs), play a crucial role in the oocyte's potential for successful fertilization and embryo development⁶. Given this, and assuming that the quality of an oocyte determines its potential for fertilization and subsequent embryo development, it is imperative to recognize the differences in the ultrastructural organization of oocytes from various donor groups.

Typically, oocyte selection for in vitro procedures is based on the general appearance of an oocyte under low magnification microscopy without a full appreciation of the ultrastructural nuances⁷. However, in species with advanced and successful assisted reproductive technologies (ART), additional factors such as donor age, health, and reproductive status are also often considered important^{7,8}. Additionally, ovarian stimulation is commonly performed before oocyte collection in many species to increase the number of available oocytes for in vitro procedures^{9,10}.

In contrast, the situation with cats is significantly different. Most in vitro procedures in feline species utilize oocytes collected from ovaries, which are medical waste from routine neutering surgeries or occasionally harvested postmortem. With recent advances in veterinary clinical practice, safe ovariohysterectomy procedures can now be performed on very young, even pediatric, cats. This, combined with the growing popularity of neutering programs aimed at reducing the stray cat population in Western countries^{11,12}, often leads to situations where gonads intended for ART are harvested from sexually immature kittens. Conversely, in wild felid species, the oocytes collected often originate from older or diseased females, which likely has an impact on in vitro performance¹³.

Furthermore, because the oocytes for in vitro use are typically selected based on their general morphology under light microscopy^{7,14}, many crucial characteristics that determine oocyte quality go unnoticed and are therefore not considered in the final classification of the gamete. These include cytoplasmic organelles that

¹Department of Reproduction and Clinic of Farm Animals, Wrocław University of Environmental and Life Sciences, Norwida 25, Wrocław 50-375, Poland. ²Department of Ultrastructural Research, Wrocław Medical University, ul. Chałubińskiego 6a, Wrocław 50-368, Poland. ³Department of Animal Reproduction, Anatomy and Genomics, University of Agriculture in Kraków, Kraków, Poland. ⁴Department of Human Biology, Wrocław University of Health and Sport Sciences, Paderewskiego 35 Avenue, 51-612, Wrocław, Poland. ✉email: natalia.anna.bragiel@gmail.com; michal.kulus@umw.edu.pl; malgorzata.ochota@upwr.edu.pl

influence developmental competence, such as the arrangement and architecture of mitochondria, lipid droplets, and cytoplasmic vacuoles, cortical granules as well as the density of microvilli. The above factors, specific to cats in terms of the random source of oocytes used in vitro, likely influence their developmental potential, thereby affecting the outcomes and potentially leading to high failure rates.

Sexual maturity and aging affect gamete quality¹⁵. At birth, ovaries have a limited number of primordial follicles¹⁶, with oocytes in early meiosis. Some follicles grow through developmental stages, but most undergo atresia. After puberty, gonadotropins rescue a few to reach the preovulatory stage¹⁷. Hormonal changes trigger meiosis, but only a subset of oocytes is recruited per cycle¹⁸.

As age advances, oocyte developmental competence declines, resulting in compromised fertility¹⁹. It was reported in humans, ovine, bovine, swine, mice, and carnivores that prepubescent oocytes exhibit good-quality cellular structures due to the absence of extensive metabolic and reproductive demands. However, they might not be as high in quality as their appearance under the light microscope might suggest²⁰. During pubescence, oocytes reach full competence, characterized by optimal organelle distribution, which allows for cytoplasmic maturation and readiness for fertilization. However, as oocytes age, they experience cellular senescence, including mitochondrial dysfunction, chromosomal abnormalities, and altered cytoplasmic composition^{17,21,22}.

To date, no studies have compared the ultrastructural architecture of domestic cat oocytes classified as good quality and obtained from prepubertal, cycling adults, and old domestic cats. Consequently, with the current level of knowledge, it remains difficult to determine how cellular organelles change throughout a female's lifespan and which might serve as reliable indicators of oocyte quality. Comparative analysis of the cytoplasmic organelle distribution among cats of various ages would provide insight into the suitability of particular donor queens for oocyte collection and their use in in vitro procedures. To address this, this study aimed to characterize the ultrastructure of high-quality oocytes obtained from cycling adult queens and compare them with oocytes from younger (prepubescent) and older (post-reproductive peak) queens.

Results

A total of 14 oocytes ($n = 14$) were examined. The oocytes collected from cycling adult donor queens served as the gold standard for comparisons in this study. The summary of ultrastructural findings is presented in Table 1. Representative images of the subolemmal region of distinctive groups are presented in Fig. 1. The middle part of the ooplasm (O) and ultrastructural details are compared in Fig. 2. The outer part of the cumulus–oocyte complex (COC), including the corona radiata (CR) and zona pellucida (ZP), is shown in Fig. 3. Summary statistics of the results are presented in Table 2.

Ultrastructural quality of oocytes collected from cycling adult donor cats

The outer region of the oocyte from mature donors had a few layers of well-defined and semi-densely packed cumulus cells (CC); the cells displayed non-uniform and irregular shapes, which contributed to the distinct

Structure	Young ($n = 4$)	Adult ($n = 4$)	Old ($n = 6$)
Corona radiata (CR)	Very well-defined, regular and compacted cells; clear borders between corona radiata and zona pellucida	Very well-defined, contains few layers of semi-densely compacted cells of non-uniform and irregular shapes	Very variable, sometimes well-defined and similar to the adult group, sometimes not present at all. ER often with noticeable dilation - not seen in other groups.
Zona pellucida (ZP)	Well-defined, regular, smooth and compacted with a moderate amount of connected and free-ended TZPs	Well-defined and regular and wide, with very many TZP of various shapes and lengths, quite often free-ended	Visibly thinner than in other groups, less TZP heterogenous, not very well visible, mostly free-ended
Perivitelline space (PVS)	Regular, well-defined	Well-visible, regular	Wider than in the rest of the groups, irregular with thinner and wider spots
Microvilli (MV)	Well-visible, abundant		Less abundant and shortened than in other groups
Cortical granules (CG)	Uniformly in the subolemmal region, dispersed, very rarely seen in cytoplasm, single or in groups of 2 or 3		
Ooplasm (O)	Darkest among all groups, uniform and granular, well-defined borders of vacuoles	Moderately light in color, with variable appearance; intracytoplasmic vacuoles are not always clearly differentiated from the surrounding cytosol	Lightest in color, and less uniform, vacuoles often exhibit partial loss of their borders, contributing to the lighter appearance of the cytosol
Lipid droplets (LD)	Mainly large in size and high in number	Mainly small to mid-sized, moderate amount present	Mainly large and high in number
Vacuoles (CV)	Similar to the adult group, with very well defined borders	Highest in number and surface area ($CV/\mu m^3$), typically clearly distinguishable from the surrounding cytoplasm	Few in number but large - tend to fuse together; frequently remnants of vacuoles blend into the ooplasm
Peridroplets mitochondria (PDM)	Mitochondria were sometimes seen around LDs, but not as often as in adult queens	High frequency of mitochondria found surrounding LDs, often in association with endoplasmic reticulum	Mitochondria were sometimes seen around LDs, but not as often as in adult queens
Golgi Apparatus (GA)	Sometimes present, but not very common	Present in large numbers, all GA observed had the trans subunit directed toward the inner cell	Present in large numbers, number of GA seem to increase with age, variable trans subunit orientation - directed towards the inner or outer cell
Mitochondria (Mt)	Dense mitochondria matrix, mostly intact	Uniform morphology and size, round shape, rarely damaged, frequently tend to cluster around other cytoplasmic organelles (LDs and CVs)	Swollen, often damaged, variable diameter, no visible pattern with regard to its distribution in ooplasm

Table 1. Age-dependent differences in oocyte ultrastructure.

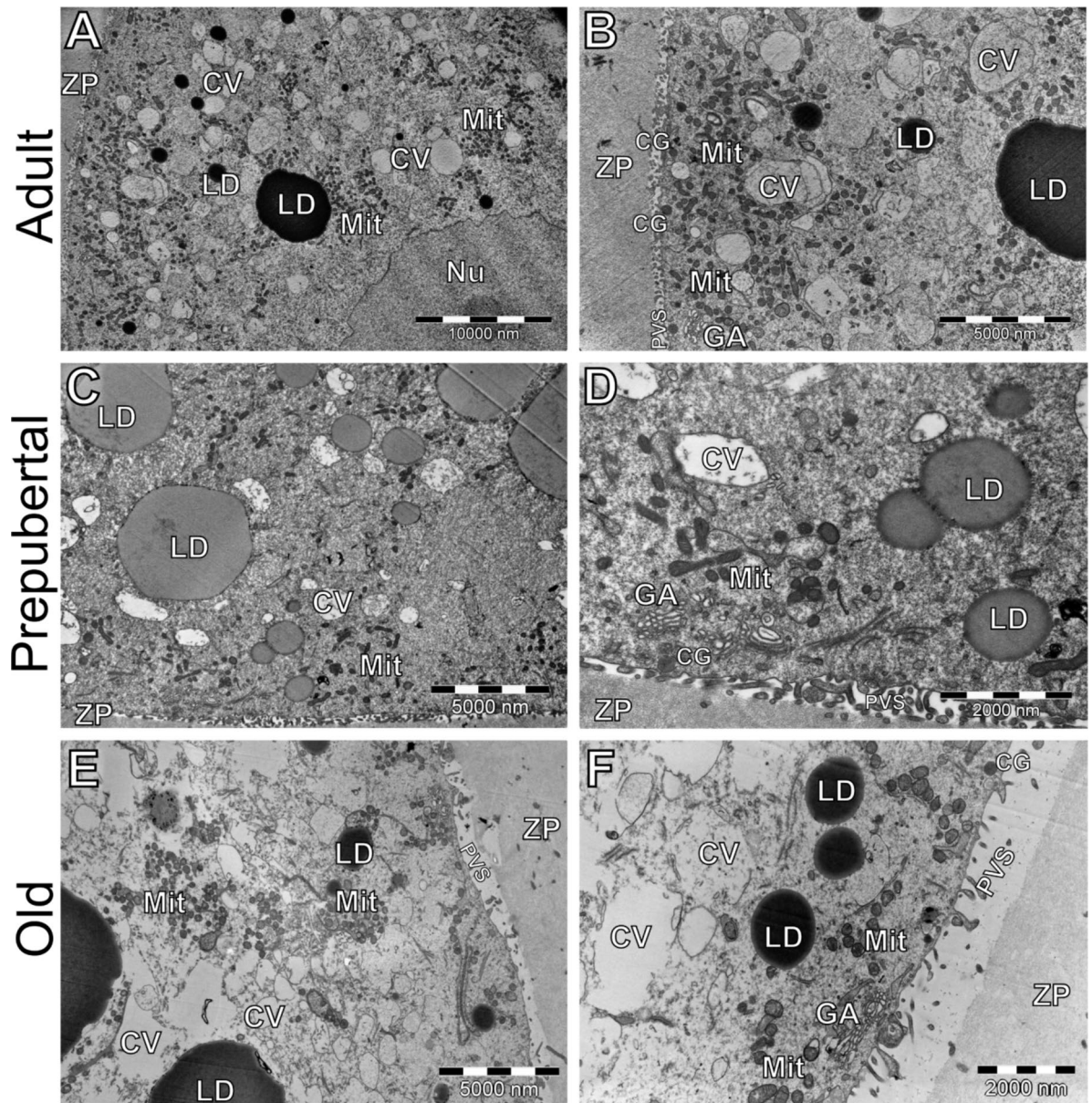


Fig. 1. Comparison of the subolemmal region of oocytes from adult (A, B), prepubertal (C, D) and old queens (E, F). Relatively small magnifications are on the left, larger magnifications are on the right. **A, B:** Adult oocytes usually show an abundance of cytoplasmic vacuoles (CV) and several small and medium-sized lipid droplets (LD). Mitochondria form clusters that aggregate around cytoplasmic vacuoles and larger LDs. The perivitelline space (PVS) is clear, narrow and distinct from the zona pelucida (ZP). **C, D:** CVs of oocytes collected from prepubertal queens tend to be less abundant. Fewer mitochondria are usually visible and do not form visible large clusters. Oocytes from old individuals (E, F) show an abundance of severely damaged CVs, the ooplasm is less distinct. Although mitochondrial clusters are present, they show no visible pattern in their distribution relative to other organelles. Microvilli are scarce, perivitelline space is uneven and relatively thick. Abbreviations: CV - cytoplasmic vacuole, CG - cortical granules LD - lipid droplet, Mit - mitochondria, GA - golgi apparatus, Nu - cell nucleus, PVS - perivitelline space, ZP - zona pelucida.

morphology of the CR. The ZP was well-defined, wide, and regular, appearing light in color and heterogeneous in texture. It contained numerous transzonal projections (TZPs) of various shapes and lengths (Fig. 3A-B).

The subolemmal region was characterized by well-defined, regular, and clearly visible perivitelline space (PVS) containing an abundance of prominent microvilli (MV) (Fig. 1B). The ooplasm of adult oocytes appeared moderately light in color with a variable appearance. Intracytoplasmic vacuoles (CV) were not always clearly differentiated and demarcated from the surrounding cytosol, leading to a more diffuse and less organized internal structure. Despite the less distinct boundaries of CV, adult oocytes contained the highest number of vacuoles (Figs. 1A-B and 4, graph A; Table 2).

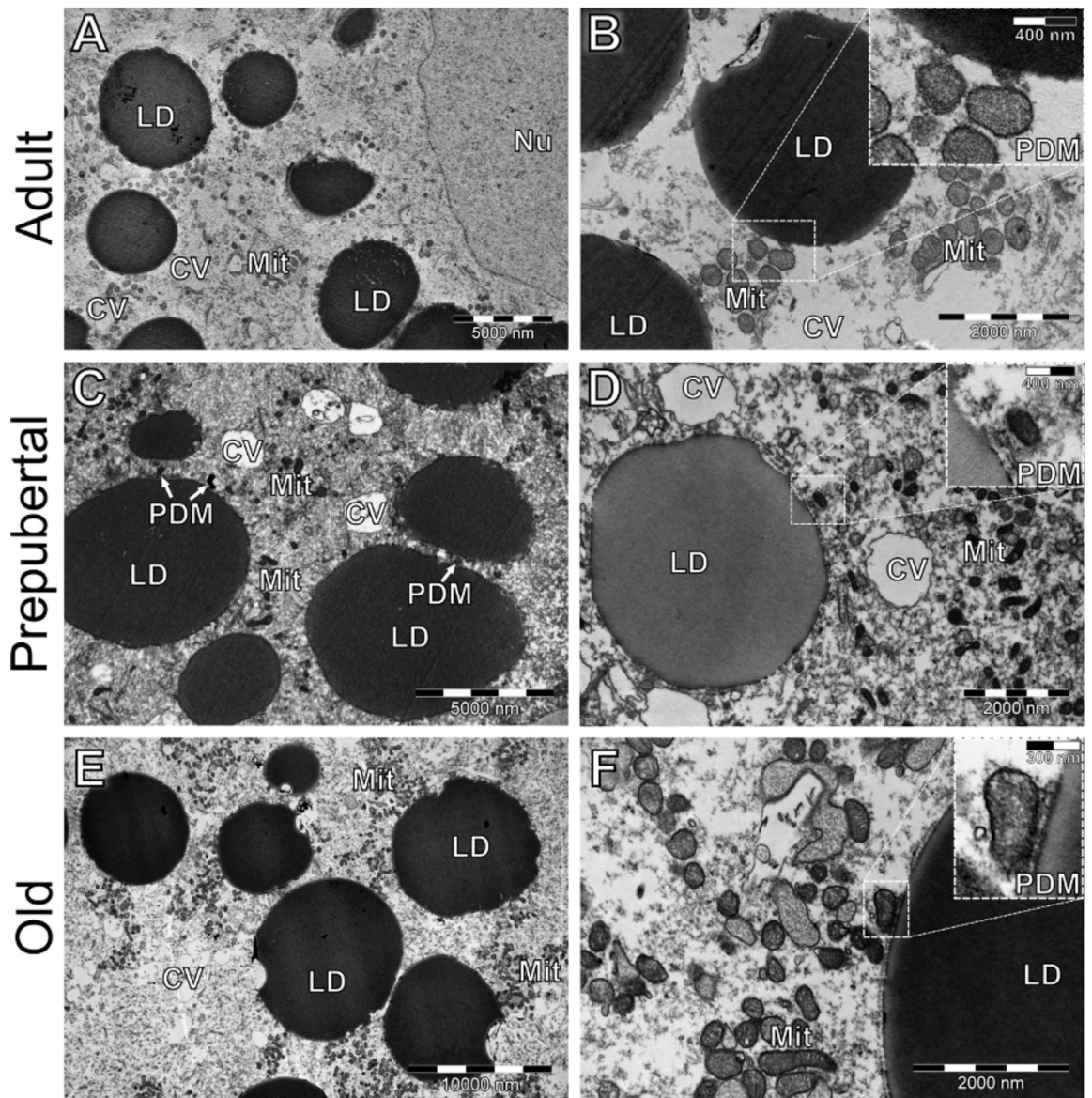


Fig. 2. Comparison of the central part of oocytes from adult (A, B), prepubertal (C, D) and old queens (E, F), focusing on the regions rich in lipid droplets. A, B: Mitochondria tend to cluster closely around LDs, possibly as peri-droplet mitochondria (PDM). In some images, a clear association between PDM and LDs is visible (see frames). C, D: Although less abundant, PDM are also visible in prepubertal oocytes. E, F: Many mitochondria are clustered in seemingly random regions of the ooplasm, although some tend to be closely associated with LDs as PDM. Abbreviations: CV - cytoplasmic vacuole, LD - lipid droplet, Mit - mitochondria, Nu - cell nucleus, PDM - peri-droplets mitochondrium.

In the inner oocyte region, there was a moderate amount of LDs, predominantly of a small to mid-sized size. A notable feature in adult oocytes was the frequent presence of Mt located near LDs. Compared to other groups, oocytes in this group had a significantly higher number of Mt in close proximity to LDs with counts as follows: young (0.24), adult (0.48), and old (0.2) number of PDM/ μm^2 of LD circumference (Figs. 2A-B and 4, graph C; Table 2). Mt present in adult oocytes exhibit a consistent morphology, typically displaying a round shape and rarely showing signs of damage. Additionally, these organelles tend to cluster around other cytoplasmic structures, such as LDs and CVs (Fig. 2B). This pattern is not observed in younger groups or in oocytes from older individuals (Fig. 2D, F; Table 2). The mean mitochondrial diameter was significantly larger in adult oocytes (243,25) compared to young oocytes (177,75), ($p < 0.05$), indicating mitochondrial maturation, while old oocytes exhibited further enlargement (257,50), likely due to swelling and structural deterioration (ANOVA $p = 0.009$) (Fig. 5A). The proportion of damaged Mt was found to remain at a relatively low level in adult oocytes (2.25), a finding which was significantly higher than in young oocytes (0,25), and markedly lower compared to old oocytes (12,25), ($p < 0.05$) (Fig. 5B). This suggests that mitochondrial integrity is largely preserved during adulthood but declines with aging (ANOVA $p = 0.028$). The mean number of cristae per Mt did not differ significantly between

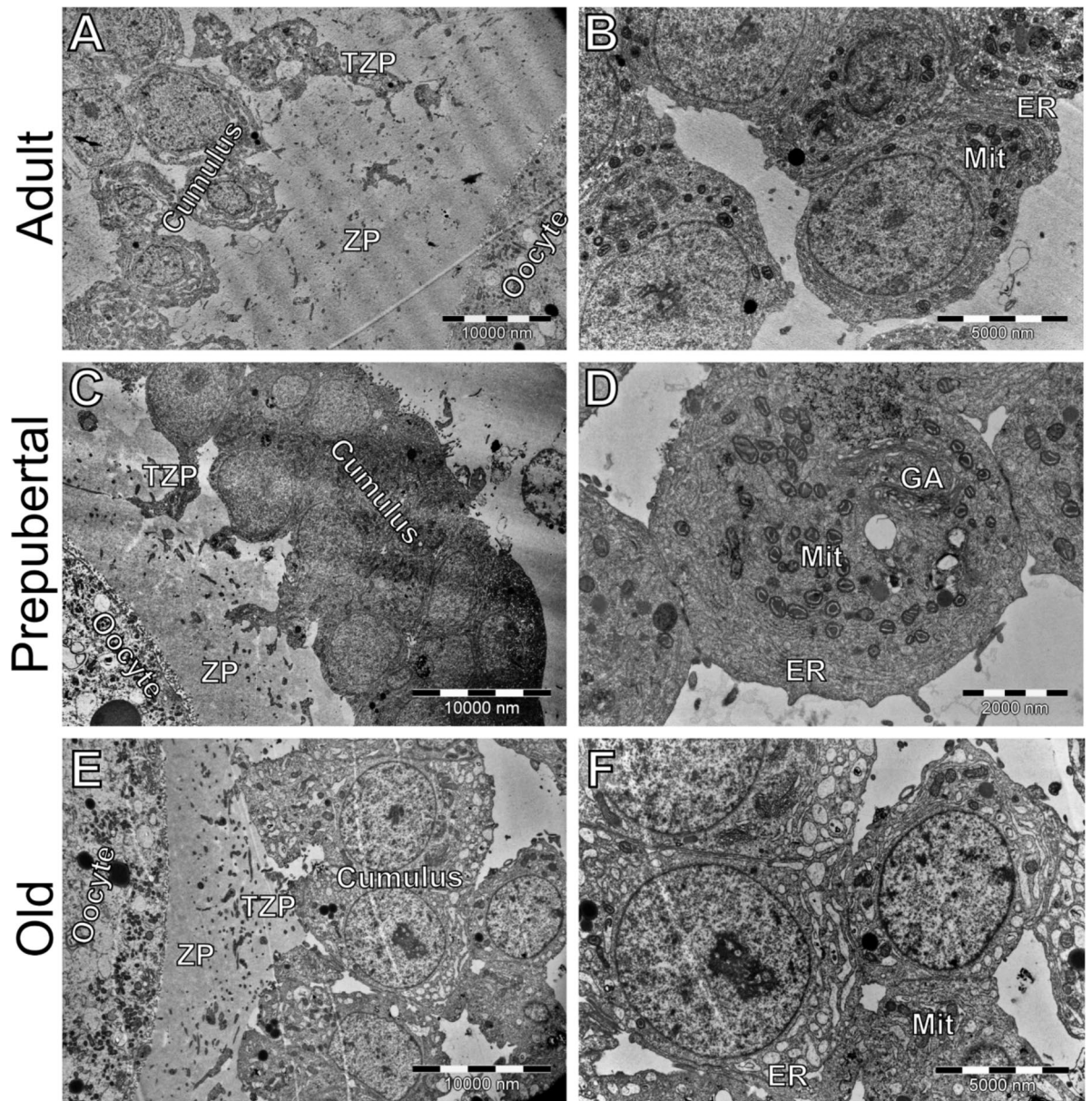


Fig. 3. Comparison of zona pelucida and corona radiata of oocytes from adult (A, B), prepubertal (C, D) and old queens (E, F). Left, low magnification; right, higher magnification focused on individual cells. The zona pelucida (ZP) tends to be widest in oocytes from adult cats (A), although the cumulus cells tend to be less densely attached than in the other two age groups. In each group, transzonal projections (TZP) originating from cumulus cells penetrate the zona pelucida toward the oolemma. Cumulus cells show a similar morphology in adult and prepubertal cats (B, D); in old cats, the endoplasmic reticulum (ER) tends to be visibly dilated.

age groups (ANOVA, $p=0.36$). The mean counts were as follows: adult oocytes (0.98), young oocytes (0.75), and old oocytes (0.87) (Fig. 5C). Similarly, this group exhibited the highest number of CV, with a count of $28.60 \text{ CV}/\mu\text{m}^3$, compared to $20.25 \text{ CV}/\mu\text{m}^3$ in the young group and $10.17 \text{ CV}/\mu\text{m}^3$ in the old group (Figs. 1A–B and 4, graph A; Table 2). The Golgi apparatus (GA) was present in large numbers within the oocytes, interestingly all observed GAs exhibited the trans subunit oriented towards the inner cell.

Ultrastructural characteristics of oocytes collected from prepubertal queens

The outer cell structures were quite similar to those in oocytes from cycling adult donors, however, the CR cells were more compact with a very clear demarcation from the ZP. The ZP was well-defined, however, contrary to adult oocytes, prepubertal oocytes were darker in color, very regular in shape and smooth, with only a moderate amount of TZPs (Fig. 3C–D).

	Mean	Min	Max	<i>n</i>
% lipid droplets				
Adult	10,89	3,98	26,31	4
Young	23,05	8,30	40,89	6
Old	15,45	9,76	24,71	4
Number of cytoplasmic vacuoles (CV)				
Adult	28,60	7,00	58,00	4
Young	20,25	8,00	42,00	6
Old	10,17	3,00	16,00	4
Number of CV/ μm^2				
Adult	0,03	0,01	0,05	4
Young	0,03	0,01	0,04	6
Old	0,013	0,00	0,02	4
Number of PDM/ μm^2 of LD circumference				
Adult	0,48	0,41	0,57	4
Young	0,24	0,14	0,41	6
Old	0,2	0,08	0,28	4
Cortical granules/ μm of oolemma				
Adult	0,50	0,28	0,70	4
Young	0,24	0,12	0,69	6
Old	0,43	0,31	0,61	4
Mean mitochondria diameter [nm]				
Adult	243,25	227	262	4
Young	177,75	144	213	6
Old	257,50	246	269	4
Fraction of damaged mitochondria				
Adult	2,25	2	3	4
Young	0,25	0	1	6
Old	12,25	2	25	4
Mean number of cristae per mitochondrion				
Adult	0,98	0,79	1,20	4
Young	0,75	0,57	0,94	6
Old	0,87	0,63	1,18	4

Table 2. Summary.

The PVS was regular and well-defined in prepubertal oocytes, similar to the well-visible and regular perivitelline space in adult oocytes. Additionally, as with adult oocytes, those obtained from prepubertal individuals exhibit well-defined and abundant Mv (Figs. 1D and 3C). The ooplasm (O) in prepubertal oocytes is notably darker and granular, with well-defined borders of CV when compared to adult oocytes. Vacuoles were similar to those in adult oocytes but exhibited more distinctly defined borders (Figs. 1D and 2C-D).

In the inner region, the LDs were predominantly large and numerous, constituting the highest percentage among the groups—in contrast to adult oocytes which had smaller and mid-sized LDs in moderate amounts (Figs. 1C, 2C-D and 4, graph B; Table 2). The peridroplet mitochondria (PDM) were also sometimes observed in prepubertal oocytes but not seen as frequently as in mature oocytes (Figs. 2C-D and 4, graph C; Table 2). In young oocytes, Mt exhibited a dense matrix and were mostly intact; however, they lacked the characteristic clustering around LDs and CVs observed in adult oocytes (Fig. 2D; Table 2). The GA is present in prepubertal oocytes but in lower numbers compared to adult oocytes.

Ultrastructural characteristics of oocytes collected from old queens

In the outermost structures, of the oocyte from aged donors, the CR showed a highly variable appearance, ranging from well-defined and similar to the cycling adult group to a reduced number of layers or complete absence, with many cells exhibiting noticeable dilation of the endoplasmic reticulum (ER), a feature absent in other groups (Fig. 3F). The ZP was visibly thinner, darker, and homogeneous in appearance with a lower number of visible TZP, contrasting with the well-defined, regular, and wide ZP of adult oocytes (Fig. 3E).

The subolemmal region consisted of the irregular PVS with thinner and wider regions, whereas it was well-visible and regular in adult oocytes. Microvilli in old oocytes were less abundant and shorter than in adult oocytes (Fig. 1E-F). The ooplasm of aged oocytes displayed the lightest coloration across all groups, likely resulting from the fusion of multiple CV, with remnants often merging into and dispersing within the ooplasm. The CV were often large but fewer in number, partially losing their borders and contributing to the lighter appearance of the cytoplasm (Figs. 1E-F and 4A).

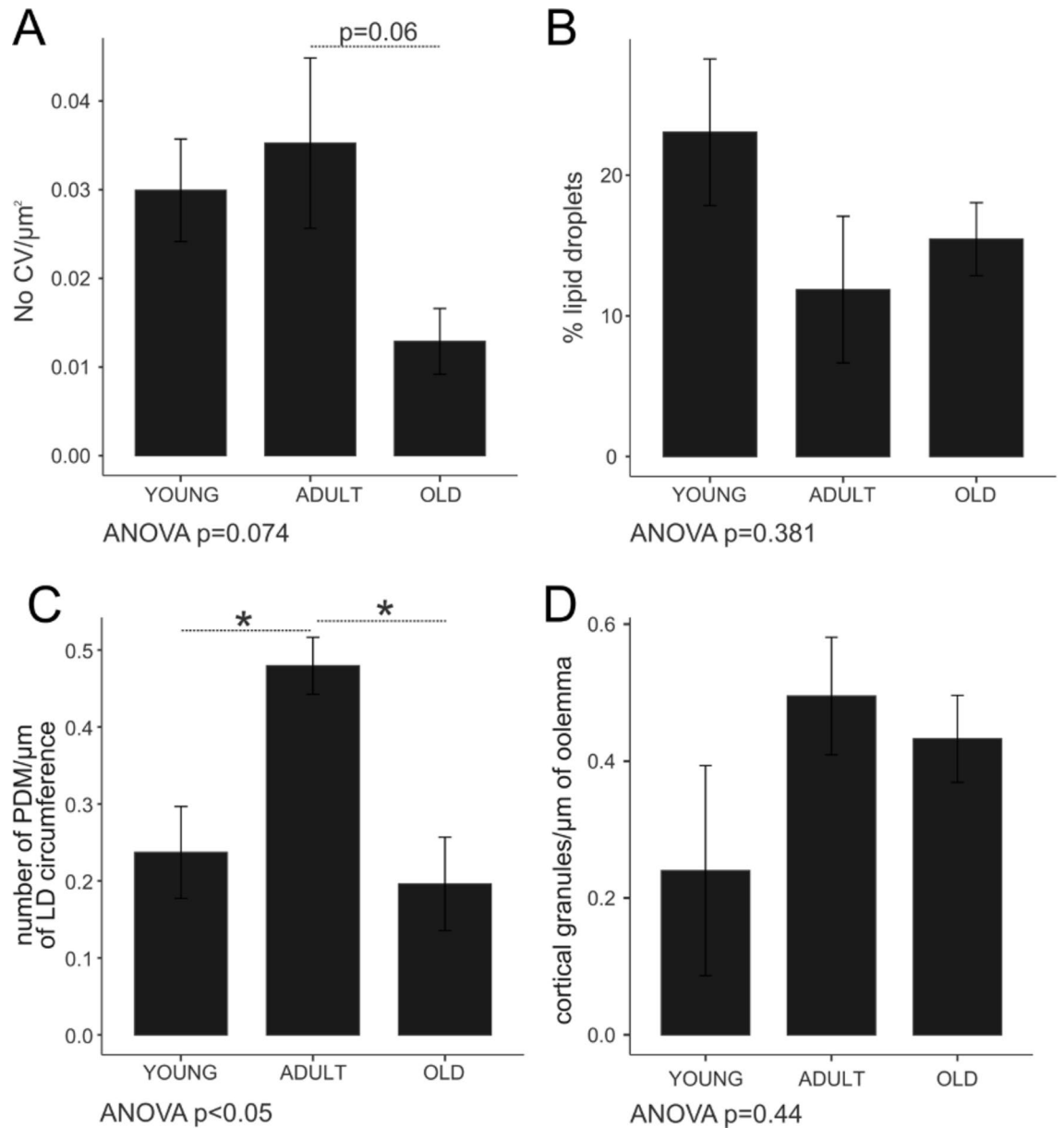


Fig. 4. Presents bar plots comparing the number of cytoplasmic vacuoles per square micrometer (A), the percentage of oocyte area occupied by lipid droplets (B), the mean number of peri-droplet mitochondria (or contact sites) per lipid circumference micrometer (C), and the number of cortical granules per micrometer of the oolemma (D). Every trait was calculated in hot-spots. In A, the results approach the statistical significance threshold, whereas in C, they are statistically significant, indicating a more dense distribution of peri-droplet mitochondria than in other groups. * - p-value < 0.05.

The inner regions of oocytes from old donors contained generally larger and more numerous LDs compared to adult oocytes (Figs. 2E-F and 4B; Table 2). The PDM were also found, but significantly less often, representing the lowest number of PDM among the groups (Figs. 2F and 4C; Table 2). In oocytes from older individuals, the Mt appeared to be swollen, frequently damaged, and exhibited a variable diameter (Fig. 2F). This is in contrast to the uniform morphology and minimal damage observed in oocytes from adult donors. Furthermore, the distribution of these organelles within the ooplasm exhibited no discernible pattern (Figs. 1F and 2F; Table 2). The GA was more abundant in older oocytes suggesting that their quantity increased progressively with age. The observed trans-subunit orientation was variable - directed towards the inner or outer cell.

Discussion

The present research aims to elucidate the ultrastructural differences in oocytes collected from female cat donors of varying ages, and classified as good quality based on light microscopy assessments. This study investigates critical aspects of oocyte architecture, including lipid droplets (LD), mitochondrial (Mt) distribution, cytoplasmic

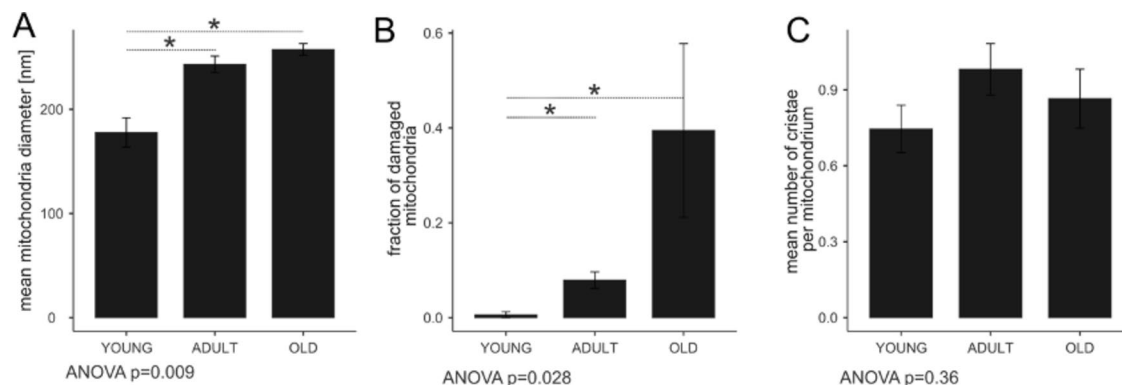


Fig. 5. The morphometric characteristics of mitochondria. Mean diameter of mitochondria (A), fraction of damaged mitochondria (B) and mean number of visible cristae per mitochondrion (C). Mitochondria in oocytes from prepubescent queens were significantly smaller and less often damaged. All mitochondria were evaluated in their cross-sections. * - p-value < 0.05.

vacuoles (CV) number, and morphology, as well as the characteristics of the oocyte's outer region, as well as encompassing the zona pellucida (ZP) and cumulus cells (CC).

Hormonal changes during puberty and each reproductive cycle significantly affect oocyte behavior and cytoplasmic organelle distribution. Studies have shown that oocytes collected from cycling females exhibit distinct patterns of organelle distribution, reflecting their developmental and hormonal status²⁷. By examining these factors, the research aims to uncover age-related variances that could impact oocyte quality and reproductive potential, providing valuable insights into the reproductive biology of female donors.

The successful development of a viable oocyte is closely linked to the preservation of energy balance within the ovarian and follicular microenvironment²². In reproductively active females, oocytes are triggered to resume meiosis, a process that demands a significant amount of energy. Therefore, energy metabolism is one of the critical factors affecting oocyte quality. It was suggested that lipids may play a role during oocyte metabolism, because the energy originating from glucose may be inadequate to meet the demands and fatty acids need to enter the mitochondria for β -oxidation (FAO) to produce additional energy to meet the demands²⁸. Research suggests that the maturation of lipid-rich oocytes (like i.e. those of pigs) seems to be particularly dependent on energy obtained from lipid metabolism^{29,30}.

It is widely acknowledged that the dark appearance of the oocyte is indicative of a substantial accumulation of lipid reserves within the ooplasm, with feline oocytes exhibiting a notable prevalence of lipid content^{14,31}. Therefore, in our study, special attention was given to complexes comprising lipid droplets and mitochondria which may be defined as peridroplet mitochondria (PDM). As previously noted, triglyceride metabolism is crucial for oocyte function. Therefore, cytoplasmic complexes that facilitate the transfer of lipid droplet-derived fatty acids (FAs) to mitochondria play a significant role in understanding cytostructural changes in cells throughout female development. Our ultrastructural observations align with these findings and additionally highlight the potential role of the PDM. It was observed that the smallest LD were present in oocytes from mature donors. Concurrently, the PDM were found to be most densely distributed around LD in this group, which suggests that adult oocytes may utilize lipids for energy production to a greater extent than oocytes from other age-groups. These findings provide support for the hypothesis that lipid metabolism is undeveloped (there are few Mt in the vicinity), which leads to larger LDs in prepubertal oocytes than in adult oocytes. It is noteworthy that larger and more numerous LD were also observed in older queens. In this instance, the presence of larger LDs is indicative of impaired lipid metabolism, as observed in oocytes with heterogeneous ooplasm. It is postulated that larger in size and clustering LDs in oocytes with heterogeneous ooplasm may indicate impaired lipid metabolism and a reduced capacity for in vitro maturation (IVM)¹⁴. In general, the presence of nonhomogeneous ooplasm (O) and the accumulation of large LD in the center of the oocyte are indicative of atresia in the cat oocyte³².

To the best of our knowledge, there is limited research on the occurrence of PDM in oocytes, and this area requires more interest and focused study. We observed a high density of PDM in adult oocytes, followed by young, and then old oocytes, which might suggest that such formations are responsible for lipid homeostasis and energy metabolism³³. This aligns with literature indicating that PDM and contact sites are integral to maintaining cellular lipid balance and energy production. The first description of the functional co-localisation of both lipid-mitochondria organelles and lipid-mitochondria-SER was reported by Kruij in 1983³⁴. They also introduced the term 'metabolic units' to describe this phenomenon. This finding was later supported by Strumey with associates, who used fluorescence resonance energy transfer (FRET) to demonstrate the true molecular-scale association in pig oocytes³⁵.

However, it has been studied in tissues with high energy demand, such as muscle or brown fat tissue³⁶ or in the corpus luteum³⁷. Co-localization of LD and Mt was noted before³⁸ as well as the crucial role of the Mt in oocyte development, quality, and aging^{1,39}. Similarly, contact sites between mitochondria and other organelles were also described, but focusing mainly on contact with ER⁴⁰. It was shown that in specific conditions (e.g. nutrient starvation) the specialized cellular network connecting LDs and Mt is present to allow for LDs to efficiently supply the fatty acids into Mt for β -oxidation⁴¹.

We observed that the number of PDM increased after the onset of puberty in the donors and decreased again with senility as indicated by the mean contact site values ($0.24 \mu\text{m}^2$ in young, $0.48 \mu\text{m}^2$ in adults, and $0.20 \mu\text{m}^2$ in old oocytes). Consequently, adult oocytes exhibited the highest number of PDM among the studied groups, suggesting increased use of lipids for energy production by oocytes of adult cats. Moreover, in our study, we often observed that PDM were also frequently associated with ER. These hotspots are crucial for the biogenesis pathway of LDs, as the synthesis of neutral lipids begins in the ER membrane⁴². It is worth noting that, according to previous publications on the exact location of specific organelles, considerable differences were seen for the SER, which was located around the CVs in good-quality oocytes²⁵. In this research, adult oocytes, which are considered the gold standard, show a similar pattern.

Our observations confirm the previously published data on the ultrastructural quality of prepubertal and adult feline oocytes reported that oocytes from prepubertal cats had a large number of LDs often associated with Mt⁴³.

Moreover, studies conducted on other species have provided further insights into the relationship between Mt and oocyte maturation. In bovines, the final maturation of oocytes occurs within the ovulatory follicle following the LH surge. During this process, Mt tend to associate with LD, and by approximately 15 h post-LH peak, these complexes are evenly distributed throughout the cytoplasm⁴⁴. In murine models, a decrease in mitochondrial abundance in the oocytes of older animals compared to young ones has been confirmed^{45,46}. Similarly, in hamsters, a significant reduction in the number of Mt and a lower frequency of clear Mt were observed in MII oocytes from older compared to younger animals⁴⁶. These findings underscore the impact of aging on mitochondrial dynamics across different species, further illustrating the complex role of Mt in oocyte quality and reproductive aging.

Physical contact between LDs and Mt plays a crucial role in adenosine triphosphate (ATP) production through mitochondrial β -oxidation⁴⁷. This interaction is not only significant in oocytes⁴⁸ but has also been observed in other fat-oxidizing tissues such as brown and white adipose tissue⁴⁹, liver, pancreas, skeletal muscle, and heart muscle⁵⁰, where PDM have been described. Some researchers describe the LD-Mt association as contact sites⁵⁰, where the surfaces of two or more organelles are directly attached via specialized tether proteins, such as PERilipin5, DGAT2, Mfn2, MIGA2. These contact sites are believed to play a crucial role in mediating the interorganellar exchange of lipids, ions, and other essential components^{51,52}. It is worth noting that Mt play also a crucial anabolic role in the synthesis of key cellular components, including amino acids, lipids, and nucleotides, which are essential for cellular growth and function. In a somewhat counterintuitive manner, PDMs are increasing the size of LDs, rather than utilizing them^{50,53}.

We speculate that in cycling adult donors, most oocytes are activated to undergo maturation. Since maturation requires a high supply of energy that glucose metabolism alone cannot provide, oocytes must utilize lipid-based sources to meet their energy demands. As a result, LD would be closely associated with Mt, and their size would decrease as their contents are actively utilized. Conversely, oocytes from prepubertal and older females were found to have larger LD and were less often surrounded by Mt. Crosier et al. also concluded that the LDs area might indicate the effectiveness of the exchange with Mt. They noted in bovine morula that the increased lipid content was associated with the decreased density of Mt suggesting that mitochondrial dysfunction may lead to increased LDs size⁵⁴. Furthermore, in bovine, it was proven that triglycerides are the key energy source during oocyte maturation, which was hampered due to insufficient ATP source when the oocytes had restricted access to fatty acids⁵⁵. Whereas delipidated mouse oocytes could synthesize and accumulate new LDs immediately afterward, these new LDs were essential for maintaining early embryo development⁵⁶. Furthermore, the study by Młodawska et al. demonstrated that the LD content in the ooplasm (O) influences the number of MII oocytes after in vitro maturation, further supporting the idea that oolemmal lipid content in feline oocytes may be related to their ability to resume meiosis¹⁴. In general, the greater the concentration of lipids, the greater the dependence of the oocytes on the energy derived from them. However, the capacity for energy production, whether derived from lipids or carbohydrates, is species-specific³⁰.

Other traits evaluated in the current study included the evaluation of suboolemmal region. The ooplasm (O) itself was darkest in prepubertal and lightest in aged oocytes. In the latter, the appearance of cytoplasm was mainly due to CV disintegration and its content blending into the O. We observed similar distortion of CV in bad-quality oocytes that were collected from ovaries stored for 48 h²⁵. During the examination of oocyte ultrastructure, a preliminary observation seemed to indicate that the GA was more abundant in older oocytes, with its quantity seemingly increasing progressively with age, but with variable trans subunit orientation - directed towards both the inner and outer cell. While in adult oocytes we observed only the trans subunit directed toward the inner cell. This arrangement suggests an increased role in protein processing, packaging, and transport within the cell, which may be indicative of heightened cellular activity or an adaptation to aging. Similar observations were made in other species⁵⁷.

In humans, it was observed that GAs were the most prominent organelles in oocytes at the early stages of maturation⁵⁸, however, the cis-trans polarity was not easily distinguishable⁵⁹. On the contrary, in non-domestic cats GAs were rarely seen⁶⁰ whereas in young mice several large GAs were located around the nucleus⁶¹ while in Siberian tiger GA were in close spatial relation to cortical granules⁵.

Cortical granules, first seen in secondary follicles, can be described as small, vesicle-like organelles containing enzymes released after fertilization. At this stage, the granules are located in close proximity to the plasma membrane of the oocyte. Their contents are released to strengthen the ZP, consequently preventing the entry to multiple sperm cells - polyspermy⁶². The CGs in the secondary follicle tend to cluster and can be distributed either localized around the GA or throughout the ooplasm⁶³; surprisingly, in domestic cats, these granules appear to be positioned in the cortical region of the oocyte even at the secondary follicular stage⁶⁴. This characteristic, together with the early arrangement of organelles in clusters, implies that the process of oocyte maturation happens earlier in domestic cats than in other species. This could be connected to their uniqueness

as a species that undergoes induced ovulation via copulation. In contrast, in cows, small clusters of cortical granules are first observed in large secondary follicle oocytes, while in non-domestic cats, the peripheral region of the ooplasm exhibits a range of cortical granules from immature to mature stages. In the current study, the observable amount and distribution of CG was similar in all age groups, as confirmed by statistical analysis (ANOVA $p=0.44$). Although adult oocytes had a slightly higher mean cortical granule density, the differences between groups were not statistically significant, indicating that cortical granule distribution remains relatively stable across age groups.

Finally, the outer region of the oocyte, including PVS, ZP, and CR was evaluated. Similar to previous reports, the PVS increased with the age of donors in our study, which is associated with both shrinkage of the oocyte and the increase in the inner diameter of ZP^{14,65}. The MV were present in all groups, but their number and quality were the best in cycling adult donors. According to Willis (1994) in horses, the number of MV increased with oocyte maturity⁶⁶. Their shape change from a long slender profile to short and bulbous after ovulation as reported in rabbits⁶⁷.

GC differed in their compactness between prepubertal, matured, and old donors. In cycling queens CCs consisted of a few layers of well-defined, semi-densely compacted irregularly shaped cells. Similar observations were made in humans and bovines⁶⁸. The quality of CC depends on the oocytes that influence their normal differentiation and function through paracrine signaling and so-called gap junctions⁶⁹. Concurrently, CC participate in oocyte maturation and affect its developmental potential by transferring small molecules into ova⁷⁰. The closeness of that communication is reflected in the ZP and TZP appearance. We observed differences in ZP character as well as in the number of TZP between donors of different ages, likely due to the reciprocal metabolic activity of CG and oocytes. Specifically, the thick, regular, and well-defined ZP became thinner and irregular with age, potentially due to the reported spontaneous activation of CG, resulting in a brittle and uneven appearance in older oocytes^{71,72}. Similarly, human studies reported that while the ZP of fresh oocytes is characterized by a granulo-fibrillar, interconnected network with pores, the ZP of aged oocytes shows signs of disintegration. This aging-related change results in a 'cobblestone-like' appearance, with narrow clusters of granulo-fibrillar material separated by clear spaces approximately 0.3 μm wide^{68,73}. Since, the number and the quality of TZP clearly reflect oocyte activity, the highest amount is expected in reproductively active queens and reduced numbers of shorter and often free-ended TZP to be seen in aged oocytes^{43,74}. This aligns with our findings, as we observed a moderate quantity of both connected and free-ended TZPs in oocytes from young queens. In adult queens, TZPs were numerous, displaying a wide range of shapes and lengths, and frequently presented as free-ended. In contrast, oocytes from aged queens exhibited a reduced number of TZPs, which appeared heterogeneous compared to adult ones, were not as clearly visible, and were predominantly free-ended. These age-associated changes in CC and TZP morphology could thus reflect reduced intercellular support mechanisms, ultimately diminishing the developmental competence of aged oocytes.

Expanding our understanding of these cytoplasmic organelles and their correlation with standard selection methods used in ART protocols could identify the primary factors affecting oocyte quality. This, in turn, could lead to advancements in fertility preservation programs and the *in vitro* techniques employed for cat species. While some studies have linked oocyte appearance with subsequent *in vitro* performance, the success rates for *in vitro* maturation, fertilization, and embryo culture of feline oocytes remain limited compared to livestock and other species such as humans or laboratory animals⁷⁵.

These findings highlight the importance of considering hormonal influences when assessing oocyte quality and developing ART protocols. By integrating these insights, the present study aims to contribute to the optimization of oocyte selection and handling techniques, ultimately enhancing the success rates of feline reproductive technologies and improving conservation efforts for endangered cat species.

Materials and methods

Unless specified otherwise, all chemicals and reagents used in this study were obtained from Sigma-Aldrich, Poland. Ethical approval was not required since the study involved cells derived from medical waste tissues, which were processed in compliance with ethical guidelines, including institutional approval (Decision no. 13/2024). The medical waste tissues used in this study were sourced from the Small Animal Reproduction Clinic following routine ovariectomy or ovariohysterectomy procedures. The tissues were anonymized and obtained under protocols that do not require explicit owner consent.

Collection and processing of oocytes

Oocytes were collected from ovaries obtained from queens of various ages undergoing routine ovariectomy or ovariohysterectomy at the owner's request. The queens were divided into three age groups: prepubescent (11–13 weeks old), mature (at least 1.5 years old), and old (more than 10 years old). Immediately following surgical removal, the ovaries were transported to the laboratory, where they were fixed and sliced in ovum pick-up medium (IVF Bioscience, Bickland Industrial Park, Falmouth, UK) to release cumulus-oocyte complexes (COC). The high-quality oocytes were used in the experiment i.e. those that were uniform, had dark ooplasm, and were surrounded by a few layers of cumulus cells²³. The selection process was conducted utilizing a stereomicroscope [Nicon SMZ1000], according to classification published by Wood and Wildt²³ solely for feline oocytes. However, in cat during the initial selection we cannot determine the exact stage of the oocyte. It is assumed that immature GV oocytes are mainly recovered from antral follicles of female cat donors²⁴.

Preparation of oocytes for ultrastructural analysis

Selected COCs were first placed in a 2.5% glutaraldehyde solution in 0.1 M cacodylate buffer (Serva Electrophoresis, Heidelberg, Germany) for 30 min before being embedded in 30 μl of 2% agarose gel drops at 37 °C. Once the agarose solidified, the oocytes were stored in a 2.5% solution of glutaraldehyde, until transferred

for further proceeding. These agarose-entrapped oocytes were processed according to Anguish and Coonrod's standard protocol with modifications^{25,26}. In brief: cells were washed four times at 4 °C in 0.1 M cacodylate buffer (Chempur, Piekary Śląskie, Poland), post-fixed with 1% osmium tetroxide (Serva Electrophoresis) in 0.1 M cacodylate buffer for 1 h 4 °C, washed again in cacodylate buffer (4 times for 5 min each at 4 °C) and dehydrated in a graded series of ethanol solutions: 30%, 50%, 70%, 90%, 96%, 100% and acetone. Subsequently, the samples were incubated overnight at room temperature in an epoxy resin acetone solution (1:1), embedded in epoxy resin blocks (Serva Electrophoresis), and solidified at 60 °C for one week.

Sectioning and staining for oocyte TEM examination

After the one-week curing period, the blocks containing COC were sectioned into semi-thin slices (600 nm) using a Power-Tome ultramicrotome. These sections were stained with a toluidine blue solution (Serva Electrophoresis). This cutting and staining process was repeated until the optimal sectioning spots were identified (about $\frac{1}{3}$ – $\frac{1}{2}$ of the oocyte thickness). Following the evaluation of the semi-thin sections, the blocks were further sectioned into ultrathin slices (60 nm) using an Ultra 45° Diamond Knife (Diatome, Nidau, Switzerland). These ultrathin sections were transferred onto rhodium-coated copper grids (Maxta form, 200 mesh, Ted Pella, Redding, CA, USA), contrasted with lanthanides RTU solution (Uranylless; Delta Microscopies, France) and lead citrate RTU solution (Delta Microscopies). The contrasted specimens were then analyzed using a JEM-1011 Transmission Electron Microscope (Jeol, Tokyo, Japan) operating at 80 kV, and images were captured with a Morada Camera (Olympus, Münster, Germany).

Experimental design and statistical evaluation

The ultrastructural cytoplasmic arrangements, individual organelle morphology, position, and inter-structure relationships were compared using Transmission Electron Microscopy among oocytes obtained from donors of 3 age groups: prepubertal (11–13 weeks-old, $n=4$), mature (at least 1-year-old, $n=4$), and old (more than 10-years-old, $n=6$). Key features such as the corona radiata (CR) with granulosa cells (GC), perivitelline space (PVS) with microvilli (Mv), ooplasm quality (O), cytoplasmic vacuoles (CV), lipid droplets (LD), mitochondria (Mt), and endoplasmic reticulum (ER) were carefully evaluated. Special attention was given to the association between LDs and Mt, as well as evaluation of mitochondria morphometrics. Complexes, where Mt were found in close proximity to LDs, were identified, evaluated separately, and termed peridroplet mitochondria (PDM).

Each COC was evaluated separately. The evaluation included both qualitative and quantitative characteristics. Each trait was evaluated in hot-spots (the region with the most abundant occurrence of evaluated structures), at magnifications ranging from 5,000x to 7,500x. Quantitative traits included (1) percentage of area occupied by LD, (2) number of CV/ μm^2 , and (3) number of PDM/ μm of LD circumference, (4) mean number of CG per μm of oolemma's circumference. All characteristics were calculated in GIMP ver. 2.10.38 and expressed as follows: (1) as the number of pixels belonging to LD divided by all pixels occupied by ooplasm, (2) the number of undamaged CV divided by μm^2 of visible ooplasm, (3) the diameter of all LDs in was summed, multiplied by π (rounded to 3.14) to calculate the total circumference of given LDs. Then, all mitochondria in close proximity (<100 nm) to the LDs were counted and divided by the total circumference of the examined LDs. (4) CG in the suboolemmal region were counted and divided by length of the visible oolemma. For the evaluation of morphometric traits in mitochondria the magnification of 15,000–30,000x in hotspots including 25–30 μm^2 of ooplasm were used. To avoid the observatory bias resulting from observations of different sectioning, only cross-sections of mitochondria were evaluated, while longitudinal sections were excluded. Evaluated traits included (1) mean diameter, (2) mean number of cristae per mitochondrion, and (3) fraction of mitochondria with visible structural damage (including significantly swollen cristae, broken membranes, and large rarefactions).

The statistical significance of differences in all groups was assessed using the ANOVA test and between different pairs of groups using the LSD post-hoc test, with the significance level at $p < 0,05$.

Data availability

The data supporting the findings of this study, entitled “Age-related changes in the cytoplasmic ultrastructure of feline oocytes”, are stored in the Department of Ultrastructural Research, Wrocław Medical University, Wrocław, Poland (50-368) and the Department of Reproduction and Clinic of Farm Animals, Wrocław University of Environmental and Life Sciences, Wrocław, Poland (50-366). The data were gathered in a laboratory setting and generated entirely by our research team. While we do not intend to make the data publicly available, we can provide access upon reasonable request to the corresponding author.

Received: 8 January 2025; Accepted: 1 April 2025

Published online: 12 April 2025

References

- Kirilova, A., Smits, J. E. J., Sukhikh, G. T. & Mazunin, I. The role of mitochondria in oocyte maturation. *Cells* **10**, 2484 (2021).
- Tukur, H. A., Aljumaah, R. S., Swelum, A. A. A., Alowaimer, A. N. & Saadeldin, I. M. The making of a competent oocyte – A review of oocyte development and its regulation. *J. Anim. Reprod. Biotechnol.* **35**, 2–11 (2020).
- Jewgenow, K., Fernandez-Gonzalez, L., Jansch, S., Viertel, D. & Zahmel, J. Brilliant Cresyl blue staining allows the selection for developmentally competent immature feline oocytes. *Theriogenology* **126**, 320–325 (2019).
- Martins, L., Fernandes, C., Minto, B., Landim-Alvarenga, F. & Lopes, M. Ultrastructural characteristics of Non-matured and *In vitro* matured oocytes collected from Pre-pubertal and adult domestic Cat ovaries. *Reprod. Domest. Anim.* **44**, 251–254 (2009).
- GjØrret, J. O., Crichton, E. G., Loskutoff, N. M., Armstrong, D. L. & Hyttel, P. Ultrastructure of oocyte maturation, fertilization, and early embryo development in vitro in the Siberian tiger (*Panthera Tigris altaica*): IVF IN THE SIBERIAN TIGER. *Mol. Reprod. Dev.* **63**, 79–88 (2002).

6. Reader, K., Stanton, J. A. & Juengel, J. The role of oocyte organelles in determining developmental competence. *Biology* **6**, 35 (2017).
7. Lemseffer, Y., Terret, M. E., Campillo, C. & Labrune, E. Methods for assessing oocyte quality: A review of literature. *Biomedicines* **10**, 2184 (2022).
8. Aguila, L. et al. Oocyte selection for in vitro embryo production in bovine species: noninvasive approaches for new challenges of oocyte competence. *Animals* **10**, 2196 (2020).
9. Howie, R. & Kay, V. Controlled ovarian stimulation for in-vitro fertilization. *Br. J. Hosp. Med.* **79**, 194–199 (2018).
10. Bó, G. A. & Mapletoft, R. J. Historical perspectives and recent research on superovulation in cattle. *Theriogenology* **81**, 38–48 (2014).
11. Spehar, D. D. & Wolf, P. J. The impact of an integrated program of Return-to-Field and targeted Trap-Neuter-Return on feline intake and euthanasia at a municipal animal shelter. *Animals* **8**, 55 (2018).
12. Levy, J. K., Gale, D. W. & Gale, L. A. Evaluation of the effect of a long-term trap-neuter-return and adoption program on a free-roaming Cat population. (2003). <https://doi.org/10.2460/javma.2003.222.42>
13. Kochan, J. et al. Comparison of the morphology and developmental potential of oocytes obtained from prepubertal and adult domestic and wild cats. *Animals* **11**, 20 (2021).
14. Młodawska, W., Maliński, B., Godyń, G. & Nosal, B. Lipid content and G6PDH activity in relation to ooplasm morphology and oocyte maturational competence in the domestic Cat model. *Reprod. Biol.* **24**, 100927 (2024).
15. Bromfield, J. J. & Piersanti, R. L. Chapter 10 - Mammalian Oogenesis: The Fragile Foundation of the Next Generation. in *The Ovary (Third Edition)* (eds. Leung, P. C. K. & Adashi, E. Y.) 157–164 Academic Press, (2019). <https://doi.org/10.1016/B978-0-12-813209-8.00010-8>
16. Zhang, T. et al. Mechanisms of primordial follicle activation and new pregnancy opportunity for premature ovarian failure patients. *Front. Physiol.* **14**, 1113684 (2023).
17. Fair, T. Follicular oocyte growth and acquisition of developmental competence. *Anim. Reprod. Sci.* **78**, 203–216 (2003).
18. McGee, E. A. & Hsueh, A. J. W. Initial and Cyclic recruitment of ovarian follicles*. *Endocr. Rev.* **21**, 200–214 (2000).
19. Armstrong, D. T. Effects of maternal age on oocyte developmental competence. *Theriogenology* **55**, 1303–1322 (2001).
20. Palmerini, M. G. et al. In vitromaturation is slowed in prepubertal lamb oocytes: ultrastructural evidences. *Reprod. Biol. Endocrinol.* **12**, 115 (2014).
21. Johnson, J., Canning, J., Kaneko, T., Pru, J. K. & Tilly, J. L. Germline stem cells and follicular renewal in the postnatal mammalian ovary. *Nature* **428**, 145–150 (2004).
22. Tatone, C. & Amicarelli, F. The aging ovary—the poor granulosa cells. *Fertil. Steril.* **99**, 12–17 (2013).
23. Tc, W. & De, W. Effect of the quality of the cumulus-oocyte complex in the domestic Cat on the ability of oocytes to mature, fertilize and develop into blastocysts in vitro. *J. Reprod. Fertil.* **110**, 355–360 (1997).
24. Tharasanit, T., Techakumphu, M. & Lohachit, C. Reorganisation of cell cytoskeleton of Cat oocytes matured in vitro. *Thai J. Vet. Med.* **38**, 9–16 (2008).
25. Ochota, M. et al. Ultrastructural changes in feline oocytes during ovary storage for 24- and 48-hours. *Theriogenology* **197**, 101–110 (2023).
26. Anguish, L. & Coonrod, S. Preparation of mammalian oocytes for transmission electron microscopy. *Methods Mol. Biol. Clifton NJ.* **957**, 213–230 (2013).
27. Stroebach, L. In vitro production of bovine embryos: revisiting oocyte development and application of systems biology. *Vitro Prod. Bov Embryos Revisiting Oocyte Dev. Appl. Syst. Biol.* **12**, 465–472 (2018).
28. Dunning, K. R. et al. Beta-Oxidation is essential for mouse oocyte developmental competence and early embryo Development1. *Biol. Reprod.* **83**, 909–918 (2010).
29. Bradley, J. & Swann, K. Mitochondria and lipid metabolism in mammalian oocytes and early embryos. *Int. J. Dev. Biol.* **63**, 93–103 (2019).
30. Paczkowski, M., Schoolcraft, W. B. & Krisher, R. L. Fatty acid metabolism during maturation affects glucose uptake and is essential to oocyte competence. *REPRODUCTION* **148**, 429–439 (2014).
31. Guraya, S. S. A histochemical analysis of lipid yolk deposition in the oocytes of Cat and dog. *J. Exp. Zool.* **160**, 123–135 (1965).
32. Wood, T. C., Montali, R. J. & Wildt, D. E. Follicle-oocyte Atresia and Temporal taphonomy in cold-stored domestic Cat ovaries. *Mol. Reprod. Dev.* **46**, 190–200 (1997).
33. Yang, M. et al. Lipid droplet - mitochondria coupling: A novel lipid metabolism regulatory hub in diabetic nephropathy. *Front. Endocrinol.* **13**, 1017387 (2022).
34. Kruij, T. A. M., Cran, D. G., Van Beneden, T. H. & Dieleman, S. J. Structural changes in bovine oocytes during final maturation in vivo. *Gamete Res.* **8**, 29–47 (1983).
35. Sturmey, R. G., O'Toole, P. J. & Leese, H. J. Fluorescence resonance energy transfer analysis of mitochondrial:lipid association in the Porcine oocyte. *Reproduction* **132**, 829–837 (2006).
36. Cui, L. & Liu, P. Two types of contact between lipid droplets and mitochondria. *Front. Cell. Dev. Biol.* **8**, 618322 (2020).
37. Przygodzka, E., Plewes, M. R. & Davis, J. S. Luteinizing hormone regulation of Inter-Organelle communication and fate of the corpus luteum. *Int. J. Mol. Sci.* **22**, 9972 (2021).
38. Milakovic, I. et al. Energy status characteristics of Porcine oocytes during *In vitro* maturation is influenced by their meiotic competence. *Reprod. Domest. Anim.* **50**, 812–819 (2015).
39. van der Reest, J., Nardini Cecchino, G., Haigis, M. C. & Kordowitzki, P. Mitochondria: their relevance during oocyte ageing. *Ageing Res. Rev.* **70**, 101378 (2021).
40. Chiaratti, M. R. Uncovering the important role of mitochondrial dynamics in oogenesis: impact on fertility and metabolic disorder transmission. *Biophys. Rev.* **13**, 967–981 (2021).
41. Herms, A. et al. AMPK activation promotes lipid droplet dispersion on deetyrosinated microtubules to increase mitochondrial fatty acid oxidation. *Nat. Commun.* **6**, 7176 (2015).
42. Hugenroth, M. & Bohnert, M. Come a little bit closer! Lipid droplet-ER contact sites are getting crowded. *Biochim. Biophys. Acta BBA - Mol. Cell. Res.* **1867**, 118603 (2020).
43. Martins, L. R., Fernandes, C. B., Minto, B. W., Landim-Alvarenga, F. C. & Lopes, M. D. Ultrastructural characteristics of non-matured and in vitro matured oocytes collected from pre-pubertal and adult domestic Cat ovaries. *Reprod. Domest. Anim. Zuchthyg.* **44** (Suppl 2), 251–254 (2009).
44. Hyttel, P., Fair, T., Callesen, H. & Greve, T. Oocyte growth, capacitation and final maturation in cattle. *Theriogenology* **47**, 23–32 (1997).
45. Kushnir, V. A. et al. Reproductive aging is associated with decreased mitochondrial abundance and altered structure in murine oocytes. *J. Assist. Reprod. Genet.* **29**, 637–642 (2012).
46. Simsek-Duran, F. et al. Age-associated metabolic and morphologic changes in mitochondria of individual mouse and hamster oocytes. *PLoS One.* **8**, e64955 (2013).
47. Pribasnig, M. et al. Extended-resolution imaging of the interaction of lipid droplets and mitochondria. *Biochim. Biophys. Acta BBA - Mol. Cell. Biol. Lipids.* **1863**, 1285–1296 (2018).
48. Shi, M. & Sirard, M. A. Metabolism of fatty acids in follicular cells, oocytes, and blastocysts. *Reprod. Fertil.* **3**, R96–R108 (2022).
49. Acin-Perez, R. et al. Recruitment and remodeling of peridroplet mitochondria in human adipose tissue. *Redox Biol.* **46**, 102087 (2021).

50. Veliova, M., Petcherski, A., Liesa, M. & Shirihai, O. S. The biology of lipid droplet-bound mitochondria. *Semin Cell. Dev. Biol.* **108**, 55–64 (2020).
51. Scorrano, L. et al. Coming together to define membrane contact sites. *Nat. Commun.* **10**, 1287 (2019).
52. Herker, E., Vieyres, G., Beller, M., Krahmer, N. & Bohnert, M. Lipid droplet contact sites in health and disease. *Trends Cell. Biol.* **31**, 345–358 (2021).
53. Spinelli, J. B. & Haigis, M. C. The multifaceted contributions of mitochondria to cellular metabolism. *Nat. Cell. Biol.* **20**, 745–754 (2018).
54. Crosier, A. E., Farin, P. W., Dykstra, M. J., Alexander, J. E. & Farin, C. E. Ultrastructural morphometry of bovine compact morulae produced in vivo or in Vitro I. *Biol. Reprod.* **62**, 1459–1465 (2000).
55. Ferguson, E. M. & Leese, H. J. A potential role for triglyceride as an energy source during bovine oocyte maturation and early embryo development. *Mol. Reprod. Dev.* **73**, 1195–1201 (2006).
56. Aizawa, R. et al. Synthesis and maintenance of lipid droplets are essential for mouse preimplantation embryonic development. *Development* **146**, dev181925 (2019).
57. Albertini, D. F. & Rider, V. Patterns of intercellular connectivity in the mammalian cumulus-oocyte complex. *Microsc. Res. Tech.* **27**, 125–133 (1994).
58. Sathananthan, A. H. *Atlas of Fine Structure of Human Sperm Penetration, Eggs, and Embryos Cultured in Vitro* (Praeger, 1985).
59. Trebichalská, Z. et al. Cytoplasmic maturation in human oocytes: an ultrastructural study †. *Biol. Reprod.* **104**, 106–116 (2021).
60. Jewgenow, K. & Stolte, M. Isolation of preantral follicles from nondomestic cats—viability and ultrastructural investigations. *Anim. Reprod. Sci.* **44**, 183–193 (1996).
61. Narita, A., Niimura, S. & Ishida, K. Ultrastructural changes of oocytes of mice with the advancement of age. *Jpn J. Anim. Reprod.* **36**, 83–87 (1990).
62. Liu, M. The biology and dynamics of mammalian cortical granules. *Reprod. Biol. Endocrinol.* **9**, 149 (2011).
63. Fair, T., Hulshof, S. C., Hyttel, P., Greve, T. & Boland, M. Oocyte ultrastructure in bovine primordial to early tertiary follicles. *Anat. Embryol. (Berl.)* **195**, 327–336 (1997).
64. Carrizo, O. A. et al. Morphometry, Estimation and ultrastructure of ovarian preantral follicle population in queens. *Cells Tissues Organs.* **191**, 152–160 (2010).
65. Sorensen, R. A. Cinemicrography of mouse oocyte maturation utilizing Nomarski differential-interference microscopy. *Am. J. Anat.* **136**, 265–276 (1973).
66. Willis, P., Sekhar, K. N. C. & Brooks, P. Fayer-Hosken, R. A. Electrophoretic characterization of equine oviductal fluid. *J. Exp. Zool.* **268**, 477–485 (1994).
67. Longo, F. J. Ultrastructural changes in rabbit eggs aged in vivo. *Biol. Reprod.* **11**, 22–39 (1974).
68. Moghadam, A. R. E., Moghadam, M. T., Hemadi, M. & Saki, G. Oocyte quality and aging. *JBRA Assist. Reprod.* <https://doi.org/10.5935/1518-0557.20210026> (2021).
69. Gilchrist, R. B., Lane, M. & Thompson, J. G. Oocyte-secreted factors: regulators of cumulus cell function and oocyte quality. *Hum. Reprod. Update.* **14**, 159–177 (2008).
70. Varnosfaderani, R. Importance of the GDF9 signaling pathway on cumulus cell expansion and oocyte competency in sheep. *Theriogenology* **80**, 470–478 (2013).
71. Goud, A., Goud, P., Diamond, M., Van Oostveldt, P. & Hughes, M. Microtubule turnover in ooplasm biopsy reflects ageing phenomena in the parent oocyte. *Reprod. Biomed. Online.* **11**, 43–52 (2005).
72. Martinova, Y., Petrov, M., Mollova, M., Rashev, P. & Ivanova, M. Ultrastructural study of Cat Zona pellucida during oocyte maturation and fertilization. *Anim. Reprod. Sci.* **108**, 425–434 (2008).
73. Weymarn, N., Guggenheim, R. & Müller, H. Cytogenetic investigations on development and degeneration of oocytes from juvenile mice. *Anat. Embryol. (Berl.)* **161**, 9–18 (1980).
74. Miao, Y. L., Kikuchi, K., Sun, Q. Y. & Schatten, H. Oocyte aging: cellular and molecular changes, developmental potential and reversal possibility. *Hum. Reprod. Update.* **15**, 573–585 (2009).
75. Sowińska, N. The domestic Cat as a research model in the assisted reproduction procedures of wild felids]. *Postepy Biochem.* **67**, 362–369 (2021).

Author contributions

Conceptualization: N.B., M.K., M.O. and J.P.; methodology: M.K., M.O.; investigation, N.B., J.P., M.K., M.O.; validation, M.K., M.O., W.M.; resources: M.P.-O., W.N.; writing—original draft preparation, N.B., M.O., M.K.; writing—review and editing, W.M., W.N.; visualization, M.K., N.B.; supervision: M.P.-O., W.N., M.O.; All authors have read and agreed to the published version of the manuscript.

Funding

The APC/BPC is financed/co-financed by Wrocław University of Environmental and Life Sciences. The publication is co-financed by the Leading Research Groups support project from the subsidy that was increased in amount for the 2020–2025 period in the amount of 2% referred to as Art. 387 (3) of the Law of July 20, 2018 on Ministry of Science and Higher Education, Poland obtained in 2019.

Declarations

Competing interests

The authors declare no competing interests.

Additional information

Correspondence and requests for materials should be addressed to B.N., K.M. or O.M.

Reprints and permissions information is available at www.nature.com/reprints.

Publisher's note Springer Nature remains neutral with regard to jurisdictional claims in published maps and institutional affiliations.

Open Access This article is licensed under a Creative Commons Attribution-NonCommercial-NoDerivatives 4.0 International License, which permits any non-commercial use, sharing, distribution and reproduction in any medium or format, as long as you give appropriate credit to the original author(s) and the source, provide a link to the Creative Commons licence, and indicate if you modified the licensed material. You do not have permission under this licence to share adapted material derived from this article or parts of it. The images or other third party material in this article are included in the article's Creative Commons licence, unless indicated otherwise in a credit line to the material. If material is not included in the article's Creative Commons licence and your intended use is not permitted by statutory regulation or exceeds the permitted use, you will need to obtain permission directly from the copyright holder. To view a copy of this licence, visit <http://creativecommons.org/licenses/by-nc-nd/4.0/>.

© The Author(s) 2025